

Rotation in the Presence of Turbulence in Large Tokamaks

B. Scott and R. Hatzky

Max-Planck-IPP, EURATOM Association, Garching, Germany

The physics determining the momentum profile in large tokamaks is an area of active research following an increase in the diagnostics and data available [1]. Rotation is often considered in terms of toroidal and poloidal components in a general MHD setting [2]. However, in a low frequency setting it is closer to the drifts picture to consider perpendicular and parallel components, with the perpendicular one given by the “state variables” represented by densities, pressures, and the electrostatic potential. The dependent state variables in a fluid model are the densities and pressures, with the total ion charge density replaced by the vorticity, representing the ExB component given by the electrostatic potential with diamagnetic components given by ion pressures [3]. The reason for this is that if the system starts out of equilibrium, the thermodynamic state variables and the parallel momentum evolve on a transport time scale, while the vorticity approaches equilibrium on a geodesic acoustic oscillation time scale [4].

The basic geodesic acoustic oscillation is the pathway by which the ExB rotation profile comes into equilibrium. In the presence of turbulence, the 2D axisymmetric flow structure is continually kicked out of equilibrium, as Reynolds stress excites zonal flow perturbations (the flow resulting from the zonal, or flux-surface averaged, component of the electrostatic potential ϕ). The reaction to these perturbations in the toroidal setting is a geodesic transient settling such that the ion flow divergence becomes zero. With all degrees of freedom excited, some of the energy goes into a parallel flow perturbation with in/out $\cos \theta$ asymmetry. The end state is zero flow divergence, so that $\sin \theta$ perturbation in pressure p is not excited, with zero up/down $\sin \theta$ asymmetry in the pressure, so that zonal vorticity $\langle \Omega \rangle$ and parallel flows u_{\parallel} are not excited. This is called “residual undamped flow” after its initial discussion [5]. However, during the oscillations the turbulence can remove energy from any of the sideband components ($\cos \theta$ in u_{\parallel} or $\sin \theta$ in p), both of which have direct energetic cascade dynamics, out of the axisymmetric sidebands and into the turbulence (nonlinearly, fluctuations \tilde{p} and \tilde{u}_{\parallel} conserve only their contributions to fluctuation free energy).

These processes form a competition for control of the eventual ExB rotation profile, both in a time-averaged sense and also in the degree to which this profile departs the neoclassical equilibrium state. In a computation this can be diagnosed through the degree to which the parallel and perpendicular linear flow divergences balance by themselves (i.e., how negligible are the nonlinearities), and how large an amplitude of the zonal vorticity in any static layers results. If the

latter is much smaller than the diamagnetic frequency evaluated at the scale of the turbulence, then they will have only moderate effect on the turbulence at best.

These processes are studied herein with a global model of gyrofluid turbulence called GEMR — GEM is the electromagnetic gyrofluid model for electrons and ions in [6], and the “R” refers to the use of global, radially dependent, geometry. Fluxtube ordering on the derivatives is relaxed. In terms of a conventional circular flux surface model, the derivative combination in nonlinear perpendicular dynamics transforms as

$$\frac{1}{r} \frac{\partial}{\partial r} \frac{\partial}{\partial \theta} \rightarrow \frac{2}{a^2} \frac{\partial}{\partial x} \left(q \frac{\partial}{\partial y_k} + \frac{\partial}{\partial s} \right) \quad (1)$$

given the field aligning coordinate transformation

$$x = r^2/a^2 \quad y_k = q(\theta - \theta_k) - \zeta \quad s = \theta \quad (2)$$

with a the minor radius and the derivatives evaluated at $\theta = \theta_k$. The radial dependence of q is retained and the $\partial/\partial s$ derivative is not ordered small. For general magnetic geometry, this is generalised using Hamada coordinates, retaining all the qualitative features [7]. For global core computations, $x = r_a \equiv r/a$ rather than its square is used to avoid loss of resolution towards $r = 0$, and the x -dependent coordinate Jacobian is retained. Due to space considerations the details of the GEM equations are left to [6]. The other main difference in GEMR is that the curvature terms are evaluated the same way; for example, the divergence of the ExB velocity becomes

$$\nabla \cdot \mathbf{v}_E \equiv -\mathcal{K}(\phi) \rightarrow \frac{c}{B_0} [\log B^2, \phi] \quad (3)$$

where the brackets denote the antisymmetric application of the derivatives in Eq. 1. Since the dependent variables include the self consistent profiles, the reduced-MHD part of the equilibrium (cf. [8]) is carried in the dependent variables, with the zonal magnetic potential $\langle \tilde{A}_{\parallel} \rangle$ perturbing the q -profile and the $\cos \theta$ sideband giving the self consistent Shafranov shift. The coordinates are adjusted accordingly. The procedure is explained in [9].

Several standard cases have been studied. The Cyclone Base Case has $n_e = 4.5 \times 10^{13} \text{ cm}^{-3}$, $T_e = T_i = 2 \text{ keV}$, $B = 1.91 \text{ T}$, $R_0 = 170 \text{ cm}$ and $a = 62.5 \text{ cm}$, with model profiles $q = 0.854 + 2.184 r_a^2$ and initial dependent variable zonal components for each species $\langle \tilde{n}_z \rangle = 0.321 \mathcal{P}(r_a)$ and $\langle \tilde{T}_{z\parallel} \rangle = \langle \tilde{T}_{z\perp} \rangle = \mathcal{P}(r_a)$ where

$$\mathcal{P}(r_a) = \frac{\Delta_a}{2} \frac{6.9}{R_a} \left[1 - \sin \left(\pi \frac{r_a - r_0}{\Delta_a} \right) \right] \quad (4)$$

with $r_0 = 0.5$, $\Delta_a = 0.8$, $R_a = R_0/a$, and a radial domain of $0.1 < r_a < 0.9$. This is in circular coordinate geometry. An alternative which is more appropriate to standard conditions in medium

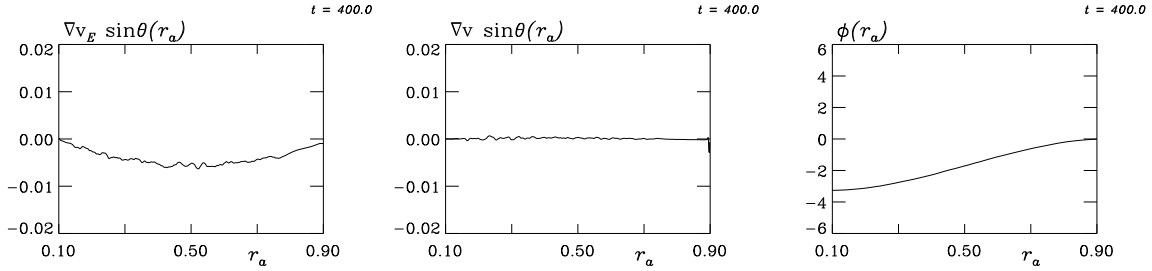


Figure 1: Ion flow sideband divergence diagnostics at $c_s t/a = 400$ for the AUG/DIV shaped divertor case with $\rho_* = 1/200$. The profiles shown are the ExB component (left) of the total $\sin\theta$ axisymmetric divergence component (center), and the resulting zonal electrostatic potential (right). This potential represents ExB rotation of the entire plasma, and it is determined by the processes which enforce the indicated ion flow divergence balance. The zonal ExB rotation profile is tightly clamped, and the zonal flow perturbations are barely visible on the ExB divergence profile.

sized tokamaks is called an AUG/DIV model. It uses a model separatrix for the boundary surface as input to the HELENA Grad-Shafranov equilibrium code [10], implemented as described in Eqs. (14–18) of [7]. The parameters are $n_e = 2 \times 10^{13} \text{ cm}^{-3}$, $T_e = T_i = 2 \text{ keV}$, $B = 2.5 \text{ T}$, $R_0 = 165 \text{ cm}$, $a = 50 \text{ cm}$, with a q profile of $1.5 + 2r_a^2$. Both models were swept in terms of $\rho_* = \rho_s/a$, from the nominal values 5.41×10^{-3} and 5.17×10^{-3} , respectively, up to $1/50$ for a smaller system and down to $1/400$ and $1/800$ for large tokamaks (these values roughly correspond to JET and ITER, respectively). The large tokamak regime is entered when the turbulence forcing upon the equilibrium, which scales as ρ_*^2 , becomes negligible compared to the neoclassical equilibration, which scales simply as ρ_* .

The results of this are always qualitatively the same. The dependent variable profiles are ramped up gradually from zero to the nominal value times \mathcal{P} over $0 < c_s t/a < 50$. The turbulence is started as a random bath of fluctuations in \tilde{n}_z (all species equal) of relative amplitude $10^{-2}\rho_*$, with all other dependent variables zero. Linearly unstable ion temperature gradient modes emerge out of this, overshooting and saturating between 100 and $200a/c_s$ later depending on the case, and then into fully developed turbulence thereafter. No sources are used, but for $\rho_* = 1/200$ and larger the relaxation is slow enough to be ignored over the length of the run, to $800a/c_s$. The ion flow divergence components are shown in Fig. 1 for the Cyclone case with $\rho_* = 1/400$ just after the most violent phase of the turbulence prior to slow decay. These are evaluated by multiplying the ion gyrocenter continuity equation (for \tilde{n}_i) by $\sin s$ and then taking the zonal average. The curvature term due to $\tilde{\phi}$ gives the toroidal divergence of the zonal component of the ExB flow. The sum of all the curvature terms including anisotropy and gy-

roradius corrections gives the ExB plus diamagnetic divergence. The linear parallel divergence is found to balance this. The total divergence neglecting the nonlinearities is tightly close to zero, indicating equilibrium balance unaffected by nonlinearities (for a contrasting picture from edge or adiabatic core turbulence see Figs. 1,2 of [9]). The fluctuating zonal flow layers themselves are barely visible on the ExB divergence profile (upper left of Fig. 1). This shows that the resulting electrostatic potential profile is set by the equilibrium and negligibly perturbed by the turbulence. This result is especially robust for electromagnetic cases, which tend towards moderately weaker turbulence than the corresponding adiabatic cases. The latter enter the large tokamak regime for somewhat larger inverse- ρ_* (cf. also the “gyro-Bohm convergence” in [11]). We have studied perpendicular flow, while u_{\parallel} is also part of the process. However, since zonal toroidal momentum varies on a transport time scale (no factors of ρ_* in its equation), the question of turbulent self-generated flows properly focusses more on the ExB rotation.

The principal result of this study, to be detailed in a forthcoming preprint, is that for large tokamaks the familiar picture of turbulence causing self-generated sheared ExB flow layers of significant amplitude ceases to hold when (1) the geodesic curvature processes are properly represented, (2) the tokamak is 200 mid-profile ion gyroradii or larger, and (3) the dynamics is electromagnetic. All three of these hold marginally in today’s medium sized tokamaks, and more so in the JET and JT-60U tokamaks where it has been observed more difficult to cause internal transport barriers than in smaller devices (in addition to increasing evidence that these barriers proceed on a transport, not a dynamical, timescale). One can be forgiven for expecting that self generated ExB flow dynamics in ITER might be of little consequence.

References

- [1] Tala T, Crombé K, de Vries P C, Ferreira J, Mantica P, Peeters A G, Andrew Y, Budny R, Corrigan G, Eriksson A, Garbet X, Giroud C, Hua M D, Nordman H, Naulin V, Nave M F F, Parail V, Rantamäki K, Scott B D, Strand P, Tardini G, Thyagaraja A, Weiland J, Zastrow K D and Contributors J E 2007 *Plasma Phys. Contr. Fusion* **49** B291–B302
- [2] Peeters A G 199x *Phys. Plasmas* **Z** zzz
- [3] Scott B 2003 *Phys. Plasmas* **10** 963–976
- [4] Winsor N, Johnson J and Dawson J 1968 *Phys. Fluids* **11** 2448
- [5] Rosenbluth M N and Hinton F L 1998 *Phys. Rev. Lett.* **80** 724–727
- [6] Scott B 2005 *Phys. Plasmas* **12** 102307 (Preprint arXiv:physics/0501124)
- [7] Scott B 2001 *Phys. Plasmas* **8** 447–458
- [8] Strauss H 1976 *Phys. Fluids* **19** 134
- [9] Scott B 2006 *Contrib. Plasma Phys.* **46** 714–725
- [10] Huijsmans G 1991 *External resistive modes in tokamaks* Ph.D. thesis Vrije Universiteit Amsterdam
- [11] Lin Z and Hahm T S 2004 *Phys. Plasmas* **11** 1099